TOXICOLOGICAL SCIENCES **123(1)**, 231–246 (2011)
doi:10.1093/toxsci/kfr165
Advance Access publication June 24, 2011

A Validated Hybrid Computational Fluid Dynamics-Physiologically Based Pharmacokinetic Model for Respiratory Tract Vapor Absorption in the Human and Rat and Its Application to Inhalation Dosimetry of Diacetyl

Eric Gloede, Joseph A. Cichocki, Joshua B. Baldino, and John B. Morris[1]

Department of Pharmaceutical Sciences, Toxicology Program, University of Connecticut, Storrs, Connecticut 06269-3092

[1]To whom correspondence should be addressed at Department of Pharmaceutical Sciences, University of Connecticut, 69 North Eagleville Road, Storrs, CT 06269-3092. Fax: (860) 486-5792. E-mail: john.morris@uconn.edu.

Received April 27, 2011; accepted June 15, 2011

Diacetyl vapor is associated with bronchiolar injury in man but primarily large airway injury in the rat. The goal of this study was to develop a physiologically based pharmacokinetic model for inspired vapor dosimetry and to apply the model to diacetyl. The respiratory tract was modeled as a series of airways: nose, trachea, main bronchi, large bronchi, small bronchi, bronchioles, and alveoli with tissue dimensions obtained from the literature. Airborne vapor was allowed to absorb (or desorb) from tissues based on mass transfer coefficients. Transfer of vapor within tissues was based on molecular diffusivity with direct reaction with tissue substrates and/or metabolism being allowed in each tissue compartment. *In vitro* studies were performed to provide measures of diacetyl metabolism kinetics and direct reaction rates allowing for the development of a model with no unassigned variables. Respiratory tract uptake of halothane, acetone, ethanol and diacetyl was measured in male F344 rat to obtain data for model validation. The human model was validated against published values for inspired vapor uptake. For both the human and rat models, a close concordance of model estimates with experimental measurements was observed, validating the model. The model estimates that limited amounts of inspired diacetyl penetrate to the bronchioles of the rat (<2%), whereas in the lightly exercising human, 24% penetration to the bronchioles is estimated. Bronchiolar tissue concentrations of diacetyl in the human are estimated to exceed those in the rat by 40-fold. These inhalation dosimetric differences may contribute to the human-rat differences in diacetyl-induced airway injury.

Key Words: **diacetyl; inhalation dosimetry; PBPK model.**

Dose response is the most fundamental concept of toxicology. The relationship between exposure concentration and tissue dose in respiratory tract targets during inhalation exposure to irritant vapors is particularly important (USEPA, 1994). Inspired vapors can be effectively removed from the airstream in proximal airways (e.g., nose, trachea, etc.) and may not penetrate significantly to more distal sites such as the bronchioles and alveoli (Medinsky *et al.*, 1999; Morris *et al.*, 2010). Thus, widely differing tissue doses are received throughout the respiratory tract during inhalation exposure. These inhalation dosimetric relationships may differ widely between rodents and man, making interpretation and extrapolation of rodent inhalation toxicity data difficult (USEPA, 1994). This is exemplified by the inhalation toxicity of diacetyl, a component of butter flavoring vapors. Exposure to high concentrations of this vapor in certain occupations has been associated with bronchial wall thickening and constrictive bronchiolitis, an inflammatory disease of the bronchioles (Akpinar-Elci *et al.*, 2004; Kreiss *et al.*, 2002). Injury to the nose and large airways occurs in rodents exposed to diacetyl, but small airway (bronchiolar) injury is minor or absent (Hubbs *et al.*, 2002, 2008; Morgan *et al.*, 2008). The degree to which inhalation dosimetric relationships contribute to this species difference in regional airway injury is not known, but Morris and Hubbs (2009) have suggested that diacetyl penetrates more effectively to the lower airways of the human than the rat. The goal of the current study was to develop an inhalation dosimetry model for the entire respiratory tract of the rat and human to facilitate quantitative inhalation risk assessment of diacetyl vapor.

The processes involved in respiratory tract vapor absorption are well understood (Medinsky *et al.*, 1999; Morris *et al.*, 2010). Airborne vapor diffuses to the air:tissue interface and, if soluble, enters the tissue phase. Once in tissue, vapor may be removed from the interface by diffusion toward the blood stream (and ultimate removal from airway tissue), local metabolism, and/or direct reaction with tissue substrates. Thus, local blood flow, metabolism, and reaction, by lowering the concentration of vapor in tissue, will serve to facilitate continued uptake of vapor from the air into tissues. Theoretically, sound models of vapor dosimetry must include descriptions of these processes. The first successful physiologically based pharmacokinetic (PBPK) model for upper respiratory tract (URT) vapor dosimetry was proposed by Morris *et al.* (1993). This model included measures of vapor solubility (blood:air partition coefficient) and local metabolism rate and

accurately described the URT uptake efficiency of a variety of metabolized and non-metabolized vapors in the rat nose. This model assumed equilibration of vapor between the air and mucus lining layers. Concurrently, Kimbell *et al.* (1993) developed a computational fluid dynamic (CFD) approach to examine URT dosimetry under non-equilibrium conditions based on engineering mass transfer theory. In a significant advance, these CFD approaches and concepts were incorporated in the PBPK model structure to form a hybrid CFD-PBPK model of URT dosimetry (Bush *et al.*, 1998). This modeling approach has successfully been applied to describe URT dosimetry of a variety of vapors in the rat and in the human nose (Frederick *et al.*, 1998, 2001, 2002; Hinderliter *et al.*, 2005; Schroeter *et al.*, 2008; Teeguarden *et al.*, 2008). In the current study, this approach was extended to include the entire respiratory tract.

The cyclic nature of breathing is an important relative to vapor uptake and should be incorporated in comprehensive models of inspired vapor dosimetry. In cyclic breathing, vapor is transferred from air to tissue during inhalation (absorption), but vapor desorbs back into the airstream during exhalation when exhaled air that has been stripped of vapor in the alveoli passes over the airways. The desorptive process can strongly affect absorption during the subsequent inspiration (Gerde and Dahl, 1991; Johanson, 1991) and leads to complex relationships between vapor solubility (e.g., tissue:air partition coefficient) and vapor uptake. The absorptive/desorptive process for human lower respiratory tract (LRT) airways was perhaps first modeled by Johanson (Johanson, 1991). This model allowed for transfer of airborne vapor into and out of anatomically defined lower airways, but did not include terms for lower airway blood flow and only modeled airway tissue as a single 15-μm thick compartment. This modeling approach was extended by Kumagai and Matsunaga (2000). Lower airway perfusion was included, but anatomically constrained tissue compartments were not nor were the large airways included in the model. Hypothetical tissue compartments were assumed, and data were fit to the model by modulating the values of the model constants. This study included a dataset (compiled from the literature) on human vapor dosimetry during mouth breathing. Included were average uptake efficiencies and end expiratory air concentrations (normalized to inspired concentration) for a variety of vapors to which the model predictions compared favorably. Tracheobronchial airways were explicitly included into a PBPK model for inspired styrene dosimetry (Sarangapani *et al.*, 2002), but the model used unidirectional constant velocity inspiratory airflow patterns and, therefore, did not include absorption-desorption behavior.

The approach for the current study was to extend the CFD-PBPK modeling structure that has been used for URT dosimetry to include the LRT and apply the model to describe diacetyl dosimetry. Toward the end, anatomically defined models for the LRT of the rat and human were developed based on the anatomical models of Yeh (Yeh and Schum, 1980; Yeh *et al.*, 1979) as described by McBride (1992). Previous publications have shown that the human and rat URT modeling structures successfully describe uptake in nose and upper airways (Frederick *et al.*, 1998, 2001; Hinderliter *et al.*, 2005; Schroeter *et al.*, 2008; Teeguarden *et al.*, 2008). The human LRT model was validated by comparison of model estimates for average uptake efficiency and end expiratory air concentrations to the dataset compiled by Kumagai and Matsunaga (2000). To provide data for validation of the rat model, two studies were performed: whole body uptake in spontaneously breathing rats of halothane, acetone, and ethanol vapor (non-reactive vapors) was measured as well as whole body uptake of diacetyl vapor (at two concentrations). The models include vapor solubility (as measured by blood:air partition coefficient), local metabolism, and direct reactivity. Therefore, the current studies included measurement of several chemical/biochemical properties of diacetyl including: blood:air partition coefficient, airway tissue enzymatic kinetics for diacetyl metabolism, and assessment of the direct reaction rate with potential tissue substrates. N-Acetylarginine was used as a representative substrate for this purpose (Mathews *et al.*, 2010). With these data, it was possible to develop a dosimetry model with no unassigned variables. The validated models were then extended to diacetyl, with the goal of comparing and contrasting the dosimetry of diacetyl to the lower airways of the rat versus the human.

METHODS

Animals and Reagents

Male F344 rats (VAF/Plus Crl:CDBR) were obtained from Charles River (Wilmington, MA). Rats were acclimated for at least 1 week prior to use and were 8–14 weeks of age at the time of use. Body weights averaged 290 g. Animals were housed over hardwood bedding in rooms maintained at 22°C–25°C with a 12-h light cycle (lights on at 0630 h). To collect tissues for the *in vitro* studies, rats were anesthetized (urethane, 1.3 g/kg) and killed by exsanguination. The entire nasal respiratory mucosa (nasoturbinate, maxilloturbinate, and anterior septum), nasal olfactory mucosa (dorsal medial meatus, ethmoturbinates, posterior septum), and extrapulmonary lower airways (trachea plus mainstem bronchi) were collected and homogenized in 3, 10, and 3 ml, respectively, of Krebs-phosphate buffer. A 0.1 g sample of the remaining lung tissue was also collected and homogenized in 10 ml of the same buffer. Homogenates were spun at 1000 × g for 5 min to remove debris and the supernatant used as described below. All reagents were the highest purity possible and were obtained from Fisher Scientific (Springfield, NJ) or Sigma-Aldrich (St Louis, MO).

In vitro *studies*

Diacetyl is known to be metabolized by dicarbonyl xylulose reductase (DCXR), a nicotinamide adenine dinucleotide phosphate (NADPH)–dependent pathway (Nakagawa *et al.*, 2002). Therefore, diacetyl metabolism was measured *in vitro* based on disappearance of NADPH. Metabolism was examined in nasal respiratory, nasal olfactory, extrapulmonary airway, and lung homogenates (total protein content of these homogenates averaged 1.6, 6.7, 2.0 and 5.5 mg, respectively). For assay, 0.1 ml aliquots of homogenate were combined with NADPH (final concentration 0.1mM) and diacetyl (0.000–15mM), in a temperature regulated (37°C) cuvette, and absorbance was monitored at 340 nm for a 10-min period. The total incubation volume was 1.0 ml. Buffer pH was 7.4. Samples without diacetyl were used as blanks. The rate of reaction was calculated from the molar extinction coefficient of NADPH

(6.22×10^3/M/cm) and was linear with time and protein concentration. Some incubations also contained 0.3mM sodium benzoate, an inhibitor of DCXR (Carbone *et al*., 2005).

The blood:air partition coefficient can be estimated mathematically from the water:air, saline:air, olive oil:air, and/or octanol:air partition coefficients. These partition coefficients were determined by vial equilibration techniques (Morris and Cavanagh, 1986). For the determinations, septum vials (40 ml) containing 0–0.4 ml water, saline, olive oil, or octanol were incubated at 37°C for 1 h or more. Headspace air diacetyl concentrations were measured by gas chromatography (see below). Partition coefficients were determined from the reduction in headspace air concentrations in the presence of known amounts of fluid assuming mass balance. Headspace air concentrations were in the 10–100 ppm range. Partition coefficient was determined with varying amounts of fluid in each vial; the measured coefficients were independent of the amount of fluid in the vial.

Reactions rates of diacetyl were determined in sealed vials. Diacetyl was incubated with Krebs-phosphate buffer (pH = 7.4), with or without the substrate N-acetylarginine at 37°C for periods of 10–60 min. N-acetylarginine concentrations of 5–30mM were used. Diacetyl concentrations were analyzed by as described below. The disappearance rate (fraction/min) was calculated by log linear regression of the fluid diacetyl concentrations.

Whole Body Uptake

Whole body vapor uptake was measured in an 8-l stainless steel and glass cylindrical chamber. Toward this end, individual animals were placed in the chamber, test compounds were added as vapors, and exposure progressed for 30 min. During exposure, air was bled out of the chamber at a flow rate of 20 ml/min and through a gas chromatograph gas sampling valve for analysis (see below). Breathing frequency was taken every 5 min by direct observation through glass port. (Carbon dioxide absorbant, e.g., soda lime, was not added because initial experiments indicated that the vapors of interest, particularly diacetyl, adsorbed.) For data analysis, plots were made of airborne concentration versus time. Log-linear relationships were observed and regression analysis was performed to calculate the rate constant for decay (fractions per minute). This was multiplied by the volume of the chamber to express decay as a clearance (liters per minute). (In initial experiments in which no rat was within the chamber, the calculated clearance was similar to the airflow sampling rate of 20 ml/min). The fractional uptake for each rat was calculated by dividing the vapor clearance (liters per minute) by the estimated ventilation rate (liters per minute) for the rat. For assessment of decay rate due to fur adsorption, etc., rats were killed by overdose with anesthetic and immediately placed in the chamber followed by measurement of decay rate for each vapor. For model validation, uptake of three non-reactive vapors was measured: halothane, acetone, and ethanol. These vapors span a wide range of blood:air partition coefficients (2.5–1800, see below). Mixtures of these three vapors were added such that the initial concentration in the uptake chamber was ~10 ppm for each. For diacetyl uptake, rats were exposed to this vapor alone. The initial concentration in the chamber was targeted to be 5 or 25 ppm; 25 ppm corresponds to concentrations used in animals toxicity testing, 5 ppm represented the lowest concentration that could be easily examined.

Analytical Methods

Airborne vapor concentrations were measured with a gas chromatograph (Model 3600; Varian, Sugarland, TX) equipped with a gas sampling valve and a 15M DB-Wax column and a flame ionization detector. Standard curves were prepared by adding known amount of compound to 4.3 l bottles, allowing > 1 h for evaporation and drawing headspace air from the bottle through the gas sampling valve. For the reaction rate studies, diacetyl concentrations were measured by high performance liquid chromatography with a Waters (Milford, MA) Model 600 pump and a Shimadzu (Columbia, MD) Model SPD-20A UV detector (wavelength 284 nm) using a Waters 3.9 × 150 mm NovaPax Phenyl column and mobile phase of 2:98 acetonitrile: 0.1% phosphoric acid (0.8 ml/min). The diacetyl peak eluted with a retention time of 2.6 min.

Statistics. Data are reported as mean ± SD unless otherwise reported. Enzyme kinetic data were analyzed by non-linear regression assuming the presence of two (Michealis-Menten) enzymatic pathways. Decay rate data were analyzed by log-linear regression. Statistical calculations were performed with Statistica software (Tulsa, OK).

Modeling

General model structure. A PBPK-CFD model for LRT vapor uptake was developed based on the tissue stack modeling approach developed by Morris *et al*. (1993), which has been used to successfully describe nasal dosimetry of diacetyl in the rat (Morris and Hubbs, 2009). This model structure has also successfully described nasal dosimetry of a variety of vapors in the rat and human (Frederick *et al*., 1998, 2001; Hinderliter *et al*., 2005; Plowchalk *et al*., 1997; Teeguarden *et al*., 2008). The model is described in detail in the Appendix. Briefly, air is allowed to pass over tissue, which is modeled as stacks of tissue compartments (Fig. 1). The most superficial compartment is the mucous lining layer, followed by epithelial and then submucosal compartments. Blood perfuses the submucosal compartments only. Vapor diffuses through the stacks on the basis of its diffusivity (Kety, 1951). The mucus diffusivity was estimated from the diffusivity of ethanol in water (Martin *et al*., 1983) and the tissue diffusivity set at a value 1/4th of the water value to account for increased viscosity of intracellular fluids (Bush *et al*., 1998; Miller *et al*., 1993; Morris *et al*., 1993). For diacetyl, mucus and tissue diffusivities were 5.2 and 1.3×10^{-4} cm^2/min, respectively. Vapor transfer from the air to the mucous lining layer (and vice versa) is modeled in accordance with mass transfer theory (Frederick *et al*., 1998; USEPA, 1994) with the overall air tissue mass transfer coefficients for the nose being obtained from the literature (see Appendix) and for the lower airways being calculated as described by Sarangapani *et al*. (2002) based on flow in circular pipes (Cussler, 1997).

Model anatomical structure. The compartmental structure of the URT portions of the respiratory tract are described in Morris and Hubbs (2009). This model consists of four tissue stacks and allows for regional ventilation patterns of the nose. Specifically, 15% of the airflow is allowed to pass over a dorsal tissue stack representing the anterior respiratory/transitional mucosa followed by a tissue stack representing the olfactory mucosa. The remaining flow (85% of total) passes over two consecutive ventral tissue stacks representing the respiratory/transitional mucosa of that region of the nose. A similar structure was used for both the rat and human models.

Lower airways were modeled similarly in the human and rat and included trachea, mainstem bronchi, large bronchi, small bronchi, bronchioles, and a gas exchange region (alveoli) in sequence. Lower airway structure and dimensions for the model were based on the model of Yeh (Yeh and Schum, 1980; Yeh *et al*., 1979) as described by McBride (1992), referred to herein as Yeh's models. Due to its length, the trachea was split into three equal length segments. The trachea and

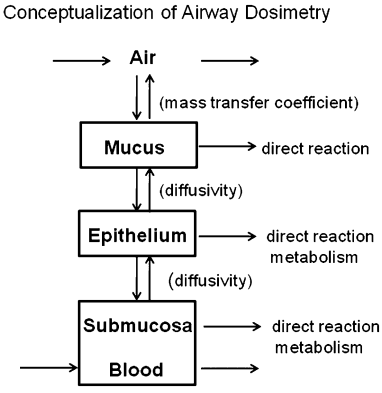

FIG. 1. Conceptual structure of airway compartmental model. Vapor in air passing over the airways is allowed to transfer into (and out of) the mucous lining layer as described by mass transfer approaches. Vapor in mucus can diffuse into tissues according to its diffusivity. Vapor can be removed from tissues by direct reactivity with tissue substrates and/or via metabolism. Vascular perfusion is allowed in the submucosal tissues only.

main bronchi were modeled as separate compartments because histopathology data are available for each of these airways (Hubbs *et al*., 2002, 2008). A lumped airway approach was used to model the bronchi and bronchioles. The large bronchi consisted of generations three to seven in Yeh's human model (McBride, 1992) and were modeled as 64 airways of 0.435-cm diameter (the number and diameter of seventh generation airways) with a total length of 2.43 cm. The length is calculated to give the same total surface area for the lumped compartment as would be obtained by summing the surface areas of individually for generations three through seven. The same approach was used to provide dimensions for the small bronchi and bronchioles. An analogous approach was used for the rat. Provided in the appendix are tables showing the airway dimensions for the human and rat model. The gas exchange region is modeled as a single compartment the volume of which varies during inspiration and expiration, with a functional residual capacity of 2700 ml for the human and 6.8 ml/kg for the rat (Kumagai and Matsunaga, 2000; Lai, 1992). The airspace within each airway or lumped airway compartment was treated as a single compartment whose volume equals the calculated volume of that airway based on its dimensions. The flow rate in each lumped airway generation was calculated by dividing the total volumetric flow rate by the numbers of airways in that generation.

The compartmental structure of the tissue stacks in the LRT model of the human is shown in Figure 2. The trachea consisted of three consecutive tissue stacks (proximal, mid, distal), but only one tissue stack is shown for the sake of simplicity. LRT tissues are modeled as stacks of 0.01-mm compartments, the total depth and distribution of cell types were based on the summary of mucosal cell types of the airways (Mariassy, 1992; Plopper and Hyde, 1992). In all airways, the most superficial layer is mucus and is modeled as a single 0.010-mm compartment. For the human LRT, the epithelium of the trachea, main bronchi, and large bronchi were modeled as four 0.010-mm compartments (total depth 0.040 mm), the small bronchi as three (total depth 0.030 mm), and the bronchioles as two (total depth 0.020 mm). An identical approach was used for the rat, except fewer numbers of 0.010-mm compartments were used for the epithelium of each airway to reflect the smaller airway thickness of this species: trachea—two 0.01-mm compartments, all other airways—one 0.01-mm compartment. In both the rat and human, perfusion occurred only in the submucosal compartments which were modeled as two 0.010-mm compartments in both species. It should be noted that the model does not incorporate the entire airway wall (e.g., smooth muscle, etc.) but only the superficial layers which are anticipated to participate in gas exchange.

Physiological parameters. Human ventilation rates are based on the ICRP dosimetry model (2001) which provides a tidal volume and breathing frequency of 750 ml and 12 breaths/min for a sitting male, and 1250 ml and 20 breaths/min for

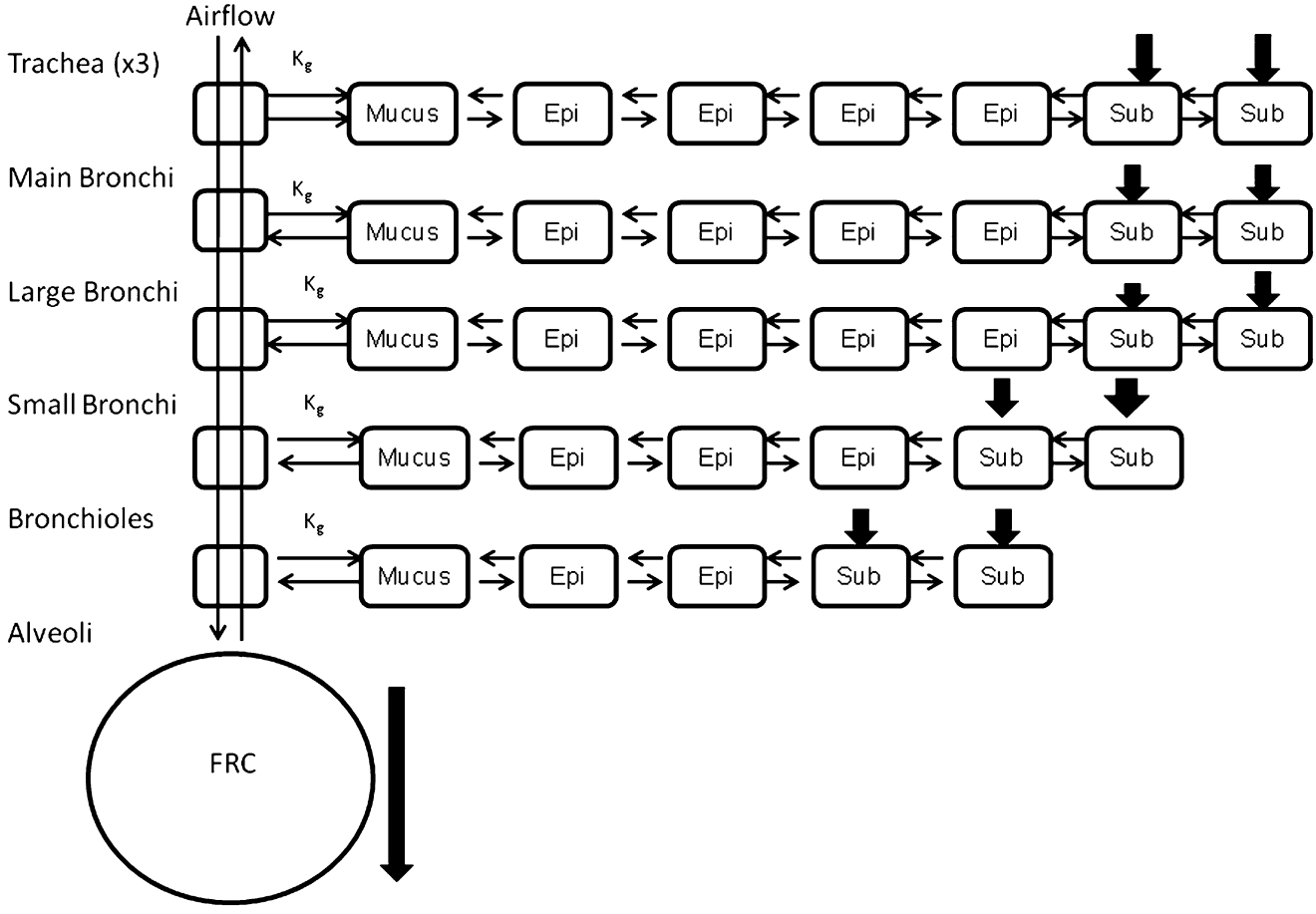

FIG. 2. Schematic representation of LRT model for the human. The thin vertical arrows represent the inspired and expired airstream. *Kg* represents the overall mass transfer coefficient for vapor between the air and tissue phase. The model consists of tissue stacks in each of multiple airways: trachea (three consecutive stacks, only one shown for sake of simplicity), mainstem bronchi, large bronchi, small bronchi, bronchioles, and alveoli. The large bronchi, small bronchi, and bronchioles represent lumped airways (see text). Each box represents a 0.01-mm deep tissue compartment (Epi = epithelium, Sub = submucosal tissue). The thick arrows indicate compartments, which are perfused. The gas exchange regions are modeled as a single compartment (FRC = functional residual capacity). An analogous structure was used for the rat with the exceptions that the trachea tissue stacks contained two 0.010-mm epithelial compartments (as opposed to the four for the human); all other airways of the rat contained one 0.010-mm epithelial compartment.

light exercise. These provide minute ventilation rates of 9000 and 25,000 ml/min, respectively. Allometric studies reveal that the tidal volume among multiple species (including human) is 7 ml/kg (Lai, 1992). Therefore, this tidal volume was assumed for the rat. The average breathing frequency of rats in this study was 130 breaths/min; this value was used for modeling efforts. Cyclic ventilation was assumed with equal time during inspiration and expiration. As in previous LRT dosimetry models (Kumagai and Matsunaga, 2000), ventilation was modeled as a square wave with inspiratory and expiratory flows equal to twice the minute ventilation.

In many species, the nose receives ~1% of the cardiac output (Brown *et al*., 1997; Frederick *et al*., 2002; Sarangapani *et al*., 2002; Stott *et al*., 1983); this value was assumed. The nasal circulation is stratified into three layers; therefore, it was assumed that one third of the total nasal blood flow perfuses the superficial capillaries which are in closest communication with the airspace. The submucosa of the LRT is perfused with bronchial circulation. The total bronchial arterial flow has been estimated to be 2% of the cardiac output (Brown *et al*., 1997; Paredi and Barnes, 2009); this flow perfuses the peribronchial plexus as well as the muscular layer of the airways and also the visceral pleura (Paredi and Barnes, 2009). It was, therefore, assumed that one-half of the total arterial flow perfuses the superficial airway tissues. Thus, the total LRT perfusion rate for the model was assumed to be one-half of the bronchial artery flow. Perfusion rates within each airway generation were assumed to be proportional to the surface area of that airway, specifically, the fraction of the total blood flow in an airway is set equal to the ratio of the airway surface area to the total surface area of all the airways. Within each airway, perfusion was assumed to be equally distributed between the two submucosal compartments. Alveolar perfusion as assumed to be equal to the cardiac output. Cardiac output was estimated based on body weight as described by Frederick *et al*. (1998).

Gas transport. Transport of vapor molecules between air and the mucous lining layer is a reversible process which depends on the vapor solubility (as measured by the mucus:air partition coefficient), concentration gradient, molecular diffusivity of the vapor in air and tissue, and the flow velocity of the airstream. It is assumed that the blood:air partition coefficient provides a reasonable surrogate for the mucus:air value (Morris *et al*., 1993). The absorption process can be described on the basis of the overall mass transfer coefficient which is dependent upon the air-phase and the tissue phase-mass transfer coefficient (MTC_A and MTC_T, respectively (USEPA, 1994). Sarangapani *et al*. (2002) provide a formula for estimating the lower airway overall mass transfer coefficient for vapors of differing partition coefficients. This approach was used. Mass transfer coefficients for nasal tissues were based on previously used values (Frederick *et al*., 1998). Transfer of vapor between the tissue compartments is described as a first order rate constant equal to the tissue diffusivity divided by the square of the depth of each compartment (Kety, 1951). It should be noted that this approach is mathematically identical to the Fick's Law-based approach used in some modeling applications (Sarangapani *et al*., 2002; Schroeter *et al*., 2008)

Diacetyl-specific parameters. α-Diketones are known to be substrates for DCXR, an enzyme that is expressed in rat and human airways (Nakagawa *et al*., 2002). Immunohistochemical studies suggest that DCXR is expressed only in the airway epithelium and is relatively evenly expressed throughout the airways of the rat (Gardiner *et al*., 2009). Therefore, it was assumed that DCXR activity was present only in the epithelium and that the activity (normalized to surface area) was uniform throughout the entire tracheobronchial tree. The enzymatic kinetic parameters obtained in the current study were used for model inputs for the rat model. It was assumed the K_m values were identical in both the rat and human. Two approaches were used for the *V*max values in the human model. In the first, the human and rat *V*max values (expressed as nmol/min/cm^2) were assumed to be identical. (*V*max is the maximal enzyme velocity; K_m is the Michealis constant, the concentration at which the half-maximal rate is observed.). The data of Nakagawa *et al*. (2002) suggest that the *k*cat for human DCXR for diacetyl is considerably lower than for the rat (1.6 vs. 25/s), therefore, the *V*max for human airways was normalized by this ratio for the second approach. (*K*cat is the overall catalytic rate and is *V*max divided by the total enzyme concentration.). A first order reaction rate constant of 0.3/min for diacetyl was used in the model (see below).

Model simulations. Human model simulations were performed for each of the vapors in the compiled dataset of Kumagai and Matsunaga (2000). The vapors in this dataset (and blood:air partition coefficients) include: desflurane (0.42), hexane (0.8), carbon disulfide (3.3), 1,1,1,-trichloroethane (3.3), dichloromethane (9.7), tetrachloroethylene (13), toluene (16), xylene (26), styrene (52), methylisobutylketone (90), methylpropylketone (150), methylethyl ketone (202), acetone (245), butanol (677), isopropyl alcohol (848), methanol (2590), ethylene glycol monobutyl ether (7970), propylene glycol monomethyl ether (12,400), ethyleneglycol monoethyl ether (22,100), and etheylenglycol monomethyl ether (32,800). Simulations were run under the ICRP estimate of 12 breaths/min with a tidal volume of 750 ml for sitting males. Uptake during a 10-min exposure was simulated. Apparent plateau values were obtained by that time. Model outputs were average overall uptake efficiency and end expiratory air concentration (normalized to the inspired concentration). Model predictions were then compared with the Kumagai and Matsunaga (2000) compiled dataset. Rat model simulation were performed for halothane (2.5), acetone (260), and ethanol (1800) (Fiserova-Bergerova, 1983; Morris, *et al*. 1986). Model simulations were also performed for diacetyl at inspired concentrations of 5 and 25 ppm.

Sensitivity analysis was performed for a vapor with blood:air partition coefficients of 500. This analysis was performed for predictions for uptake efficiency because this is the value to which the model was validated. For this purpose, each parameter was increased by 10% from its original value and the resulting change in predicted uptake efficiency was calculated and expressed as a normalized value. Thus, a 10% proportional change in uptake efficiency or penetration to the bronchioles would represent a 1:1 or 100% relative sensitivity with the parameter of interest. A positive value indicates uptake efficiency increased as the parameter of interest was increased, a negative value indicates the uptake efficiency decreased.

RESULTS

Partition Coefficients

The water:air and saline:air partition coefficients were virtually identical; the average pooled value was 572 ± 42 (mean ± SD). The octanol:air and olive oil:air values averaged 499 ± 57 and 238 ± 24 (mean ± SD), respectively. Meulenberg *et al*. (2003) and Poulin and Krishnan (1995) provide somewhat differing algorithms for estimating blood:air partition coefficient from these parameters. Human blood:air partition coefficients of 512 and 461 are estimated, and estimated rat values of 480–535 are estimated using these algorithms, respectively. A value of 500 was therefore used for subsequent modeling of diacetyl.

Metabolism Reaction Rate Studies

In vitro metabolism rates were not consistent with a single enzymatic pathway but appeared to reflect two pathways, one of high affinity and low capacity, the other of low affinity and high capacity. This pattern was seen in homogenates of all tissues: nasal olfactory mucosa, nasal respiratory/transitional mucosa, extrapulmonary airways, and lung parenchyma. Similar K_m values were observed for these pathways in all tissues. The overall averages for the K_m values in all tissues were 10 ± 2 and 6500 ± 780 nmol/ml (mean ± SEM), respectively, for the high and low affinity pathways. The calculated *V*max values for respiratory tissues are shown in Table 1. Data are provided on a whole tissue basis and on a per surface area basis (for use in the modeling). A large degree of inter-animal variability was

observed. In the respiratory/transitional, extrapulmonary, and parenchyma samples the overall activity, when normalized to surface area, appear to be similar. Therefore, average normalized values of 4 and 20 nmol/min/cm^2 was used in the modeling efforts. The DCXR inhibitor sodium benzoate (Carbone *et al.*, 2005) diminished the diacetyl metabolism rate by 25–50% when measured at a substrate concentration of 0.2mM. No greater inhibition was observed at a substrate concentration of 20mM, providing evidence that the low K_m pathway was sensitive to benzoate inhibition, but the high K_m pathway was not.

The reaction rate constant of diacetyl with N-acetylarginine was examined by measuring the rate of disappearance of diacetyl during 0 to 60-min incubation with varying concentrations of N-acetylarginine. The disappearance rate was log-linearly related to time. The pseudo-first order reaction rate constant was quite low, averaging less than 0.01/min even at N-acetyl-arginine concentrations of 30mM. (Similar values were observed using rat nasal mucosal homogenates, data not shown.) This would correspond to a pseudo-first order rate constant of 0.3/min if tissue substrate concentrations were 1M. This value (0.3/min) was included in the modeling efforts. (As noted below, inclusion of this direct reaction rate term does not substantively model estimates.)

Uptake Studies

In studies using an empty uptake chamber, the removal rate of all vapors, expressed as a clearance, was similar to the airflow sampling rate of 20 ml/min. The measured clearance rate was higher when the uptake chamber contained a dead rat, but for all vapors, the values with living animals in the uptake chamber exceeded that of dead animals by at least threefold. After correction for the value obtained with dead animals, fractional uptake values of 0.239 ± 0.03, 0.33 ± 0.03, and 0.60 ± 0.16 (see Fig. 5) were observed for halothane, acetone, and ethanol respectively ($n = 7$). Non-reactive non-metabolized vapors such as halothane, acetone, and ethanol exhibit linear first order kinetics, therefore, uptake of these vapors was not measured at multiple exposure concentrations. The average breathing frequency was 129 breaths/min. Whole body uptake of diacetyl was measured in two exposure concentration groups. In the low concentration group, the initial concentration averaged 5.2 ± 0.6 ppm and fractional uptake averaged 0.78 ± 0.11 ($n = 4$); in the high concentration group, the initial concentration averaged 22.4 ± 3.1 ppm and fractional uptake averaged 0.62 ± 0.16 ($n = 5$). Breathing frequency averaged 137 in these rats. Breathing frequencies remained constant throughout the 30-min measurement period.

TABLE 1
***In Vitro* Metabolism Kinetics for Diacetyl**

	High affinity *V*max		Low affinity *V*max	
Tissue	nmol/min	nmol/min/cm^2	nmol/min	nmol/min/cm^2
Olfactory	75 ± 16	13 ± 2	875 ± 180	154 ± 32
Respiratory transitional	21 ±14	3.9 ± 2	62 ± 17	11 ± 4
Extra-pulmonary	23 ± 9	5.5 ± 2	175 ± 93	42 ± 22
Parenchyma	226 ± 57	4.1 ± 2	391 ± 315	7.2 ± 6

Note. Data are presented as mean ± SD ($n = 4$–5) for four tissue samples, olfactory mucosa, anterior nose (respiratory plus transitional mucosa), extrapulmonary airways (trachea plus mainstem bronchi), and the remaining lung parenchyma. *V*max (maximal velocity) data were obtained by non-linear regression analysis of the *in vitro* metabolism rate data. To express per unit surface area, the activities were normalize to the surface areas predicted for each region by the model (see text for details).

Model Predictions and Validation

Shown in Figure 3 is a simulation of the concentration of a non-reactive non-metabolized vapor (blood:air partition coefficient 500) in the upper trachea and bronchioles of the human during the first 3 min of exposure at a concentration of 1 ppm under mouth breathing. Airborne vapor concentrations increase and decrease with each inspiration and expiration, respectively. It can be noted that the concentrations in the small bronchi are considerably lower than the trachea, reflective of vapor extraction in the proximal airways. Qualitatively analogous relationships were obtained in simulations for the rat. Initially, vapor concentrations in the bronchioles are quite small and build up to an apparent plateau within 1–2 min. The concentration depicted for the upper trachea during exhalation represents the concentration exhaled from the body (under the assumption of no significant absorption/desorption in the mouth). The lowest level represents the end expiratory level. In this instance, it is 32% of the inspired concentration. Calculation of the average concentration during exhalation and comparison to the exposure concentration can be used to calculate the average uptake efficiency of

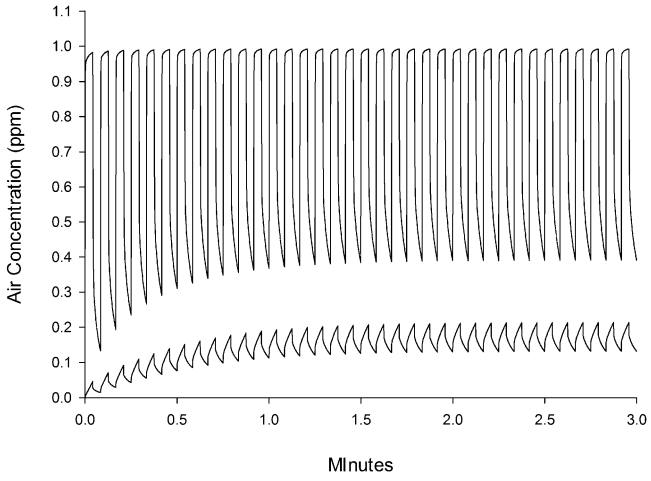

FIG. 3. Model output vapor concentration in the air in the top of the trachea (upper curve) and the air in the bronchioles (bottom curve) during 3-min exposure to 1 ppm of a non-reactive, non-metabolized vapor with blood:air partition coefficient of 500. Airborne vapor concentrations increase during inhalation and decrease during exhalation. Plateau values are achieved in ~1 min.

the respiratory tract. In this instance, an average respiratory tract uptake efficiency of 57% is calculated.

Shown in Figures 4A and 4B are the human model outputs for LRT average uptake efficiency and end expiratory air levels (during mouth breathing) for the vapors in the dataset of Kumagai and Matsunaga (2000) assuming a breathing frequency of 12 breaths/min and a tidal volume of 750 ml. Predictions are plotted versus the partition coefficient. As can be seen, a complex relationship exists between these parameters and partition coefficient. The model captured this behavior. Model estimates showed close concordance with the measured values for both uptake efficiency and end expiratory air levels. The goal of this project was to develop a first-principles, anatomically constrained model for vapor dosimetry. Therefore, no attempt was made to vary parameters to obtain a best fit.

Shown in Figures 5A and 5B are the model output and measured values for isolated URT uptake (Fig. 5A) and whole animal respiratory tract uptake (Fig. 5B) of several vapors in the

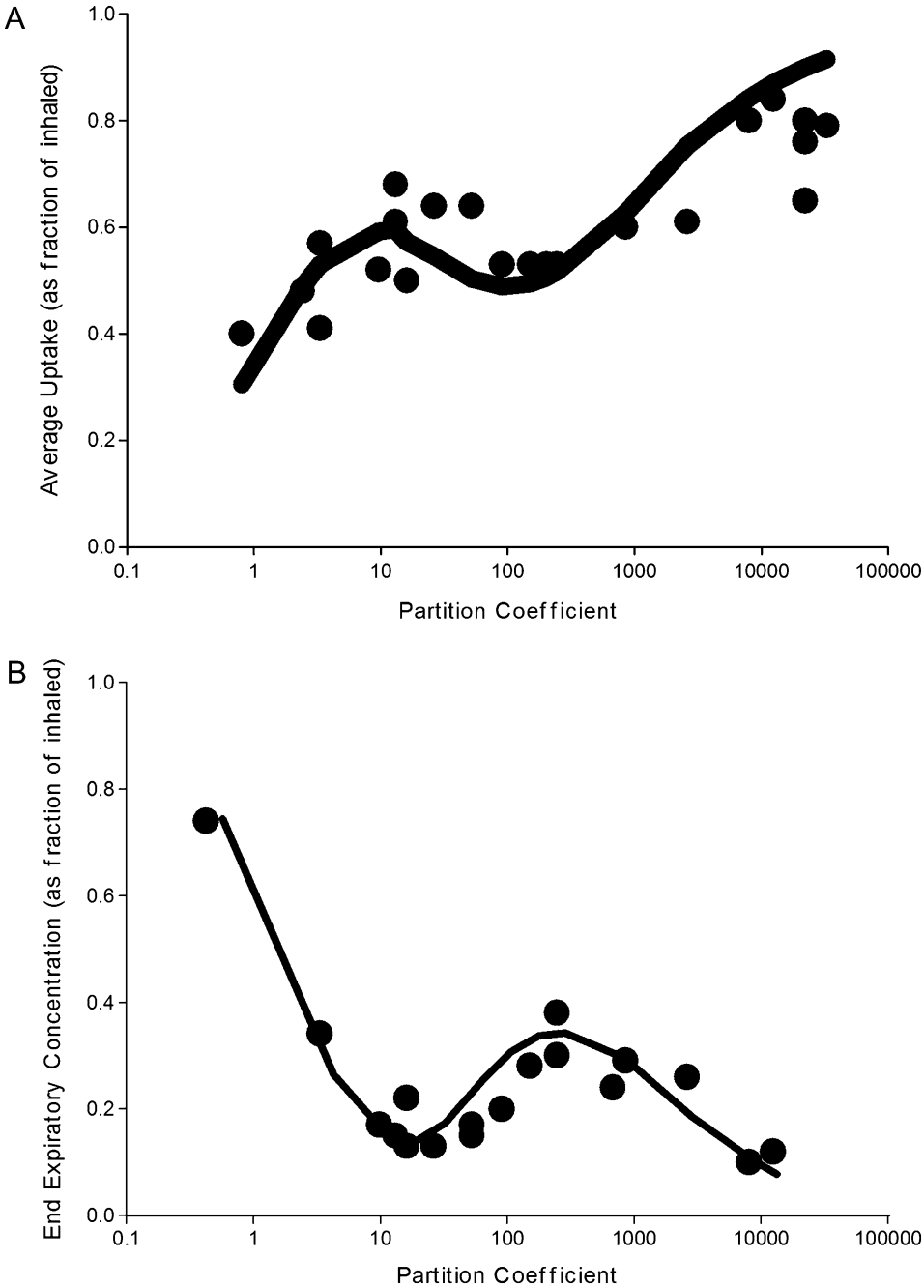

FIG. 4. Model output and measured values for LRT vapor uptake in human. Measured values are depicted as filled circles, model estimates are shown by the solid line. (A) Average uptake values for the LRT. (B) End expiratory air concentrations for the LRT expressed as a fraction of the inspired concentration.

rat. The isolated URT uptake values were obtained from our previous publications (Morris and Buckpitt, 2009; Morris *et al.*, 1993) and, for metabolized vapors, were obtained in animals pretreated with metabolism inhibitors to minimize the confounding influence of local metabolism. The strong concordance of the model estimates for isolated URT uptake provides evidence that the model structure is predictive of vapor dosimetry within an isolated airway. A concordance between model estimates and total uptake in spontaneously breathing rats is also apparent (Fig. 5B), with the predicted values being within 1 SD of the measured values. Diacetyl uptake appeared to exhibit non-linear kinetics with higher uptake efficiency at 5 ppm compared with 25 ppm. Although estimates for diacetyl uptake were somewhat lower than the measured values, the model predicted non-linear kinetics with slightly higher uptake efficiencies at 5 ppm compared with 25 ppm. To examine this in more detail, model simulations were performed under varying assumptions relative to *in situ* metabolism rates. Specifically, the model was run with metabolic *V*max values set to zero, in this condition, the model estimates uptake efficiencies of 41% at 5 and 25 ppm, values much lower than estimated when metabolism is allowed. This comparison suggests *in situ* metabolism is important in controlling overall uptake of diacetyl. Were the *in situ* metabolism rate to be twofold higher than that estimated from the *in vitro* data, uptake efficiencies of 72 and 59% would be predicted at 5 and 25 ppm, respectively.

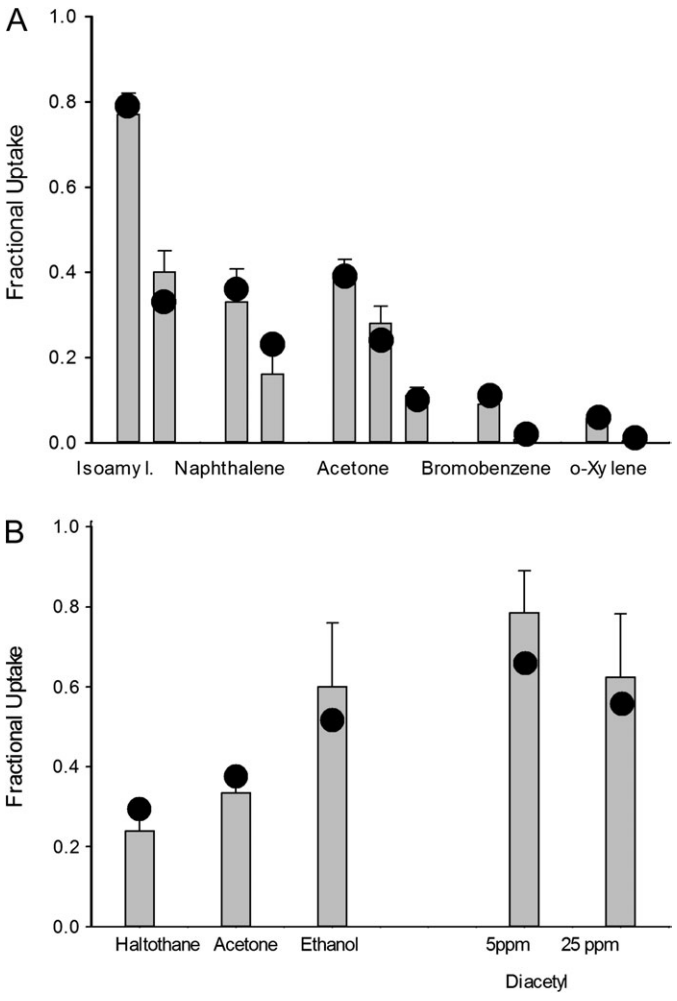

FIG. 5. Model output and measured values for vapor uptake in the rat. Measured values are depicted as bars (withSDs), model estimates are shown as filled circles. (A) Uptake efficiency in the surgically isolated URT of the urethane-anesthetized rats. (B) Whole body uptake of spontaneously breathing non-anesthetized rats.

Sensitivity Analysis

The results of the sensitivity analysis for the model are shown in Table 2. This was performed for a vapor with blood:air partition coefficient 500 and was performed assuming no respiratory tract metabolism occurred. Sensitivity analyses were performed for the nose-breathing rat, nose-breathing human, and mouth-breathing human. Effects of changing lower airway-specific parameters in the nose-breathing human may be diminished by nasal modification of the expired airstream, thus, examination of these parameters under mouth breathing allows for assessment of their importance relative to LRT disposition. Estimated uptake efficiency was most sensitive to breathing frequency, airway dimensions, cardiac output, regional airway blood flow rates, and the overall mass transfer coefficients. The sensitivities of model estimates to these

TABLE 2
Sensitivity Analysis: Relative Sensitivity Coefficients for Changes in Predicted Uptake Efficiency Caused by a 10% Increase in Each Identified Parameter

	RAT Nose breathing	HUMAN Nose breathing	HUMAN Mouth breathing
Breathing frequency	−12%	−13%	−10%
Tidal volume	−3%	−9%	−1%
Functional residual capacity	+0%	+0%	+0%
Airway length	−7%	−14%	−18%
Airway diameter	−11%	−29%	−25%
Cardiac output	+17%	+11%	+14%
Airway blood flow			
Nasal	+13%	+3%	—
Tracheobronchial	+5%	+11%	+14%
Overall mass transfer coeficient			
Nasal	−8%	+1%	—
Tracheobronchial	−5%	−10%	−12%
Tissue diffusivity	+4%	−6%	+5%

Note. Shown is the relative sensitivity in uptake efficiency caused by a 10% change in each parameter normalized to that 10% change, e.g., if uptake efficiency was increased from 30 to 31.5% this would be as a 5% increase due to the 10% change or a relative (normalized) sensitivity of 50%. A positive sign indicates that uptake efficiency was increased by increasing the parameter of interest; a negative sign indicates that uptake efficiency decreased. Sensitivity analyses were performed at an inspired concentration of 1 ppm assuming there was no respiratory tract metabolism.

parameters were generally similar for the rat and human. It should be recognized that this analysis is specific to a vapor of partition coefficient 500. (When simulations were performed including diacetyl metabolism rates, sensitivity analyses showed the same general patterns, except that the absolute magnitude of the changes caused by modulating each individual parameter was smaller, reflective of the fact that uptake was due to metabolism in addition to partitioning into tissue and removal via the bloodstream.)

Diacetyl Dosimetry

Scrubbing of vapors in proximal airways leads to decreased distal penetration of airborne vapor to distal airways. Shown in Figures 6A and 6B are the model estimated penetration fractions through each airway, in the rat and human, respectively. In the absence of metabolism, 50–60% of inspired diacetyl is estimated to penetrate through nose of the rat ('Nose' in Fig. 6A) with 20–30% penetrating through the small bronchi ('SB' in Fig. 6A) and entering the bronchioles. When metabolism is allowed, the distal airway penetration depends on the concentration, with increased distal penetration occurring at the high concentration compared with low concentration. This is likely due to saturation of the metabolic pathways (see below). At 1 ppm, only limited distal penetration of diacetyl occurs. Model estimates suggest only 20% of inspired diacetyl penetrates through the nose and less than 2% penetrates through the small bronchi and enters the bronchioles of the rat.

The model estimates that the human airways scrub diacetyl less efficiently than the rat leading to greater distal penetration. The distal penetration estimates depend on the breathing pattern. Shown in Figure 6B are the distal penetration estimates for a human breathing 1 ppm diacetyl under three conditions: nose-breathing at rest, mouth-breathing at rest, and mouth-breathing during light exercise. These simulations were performed assuming the human metabolism rate (nmol/min/cm^2) was identical to the rat. (Similar results were obtained if the *k*cat normalized metabolism rates were utilized.) Under nose breathing, the model estimates that 70% penetrates through that site and 8% penetrates through the small bronchi to the bronchioles. This is in contrast to less than 2% penetration through the small bronchi in the rat (see above). These penetration values are slightly increased during mouth breathing, but greatly increased during light exercise. Under light exercise, the model predicts that 24% of inspired diacetyl penetrates through the small bronchi to the bronchioles, a level ~10-fold greater than estimated for the nose-breathing rat. It can be noted that metabolism also appears to be important in influencing distal penetration of diacetyl in the human respiratory tract as model estimates with *V*max values set to zero estimate significantly greater distal penetration that that shown in Figure 6B. Specifically, in the absence of metabolism, it is estimated that 70% penetrates through the nose and 10% penetrates through the small bronchi and enters the bronchioles. Less than 10% is estimated to penetrate through the bronchioles to the alveoli.

The model output also provides estimated tissue concentrations during inhalation exposure (Table 3). Rat simulations were performed with metabolism rates set to zero and also using the measured enzyme kinetic parameters for the rat. For the human, simulations were performed with metabolism set to zero, assuming the *V*max (per unit surface area) was identical in the rat and human, and also assuming a *k*cat normalized *V*max (per unit surface area) to account for the potential differences between human and rat DCXR. This was performed for the high affinity pathway only. Estimated tissue concentrations were sufficiently low (< 20μM at 1 ppm diacetyl) that the low affinity pathway ($K_m = 6500\mu M$) would not be anticipated to be quantitatively important. These simulations estimated that in the absence of *in situ* metabolism roughly a 10-fold gradient would exist in diacetyl concentrations in the nose (12μM) versus the bronchioles (1μM) of the rat. This difference is a reflection of the high partition coefficient of diacetyl. In the absence of metabolism, the estimated tissue levels of diacetyl in the nose of the human are fairly similar to those for the rat and were in the low micromolar range. This was not the case for the lower airways. Due to the increased distal penetration of diacetyl in the human (see above), the concentrations of diacetyl estimated for the lower airways of the human are roughly twice that predicted for the rat.

Inclusion of metabolism enhanced scrubbing and diminished penetration (see above). The result being that the estimated concentration in the bronchiolar epithelium of the rat (0.002μM) was negligible compared with the 5μM estimated for the proximal nose. Metabolism was included in the human model by two approaches, either by direct *V*max–*V*max (per surface) area extrapolation or by basing the species extrapolation on the *k*cat values published for DCXR in the rat and human (Nakagawa *et al*., 2002). Similar results were obtained by either approach. For nose-breathing humans at rest, the estimated bronchiolar epithelial tissue concentrations are 0.008–0.011μM, exceeding those in the rat by roughly fivefold. For mouth-breathing humans at rest, similar results are obtained, with roughly a sevenfold difference predicted for the human versus rat. The differences between the human and rat are more marked under light exercise and mouth breathing. In this case, distal airway penetration is greatly increased leading to greater dose delivery to the small airways (see above). The model estimates that the small bronchi and bronchiolar tissue concentrations in the mouth breathing-lightly exercising human exceed those in the nose breathing rat by 20- to 40-fold. In fact, the estimated tissue concentration in the bronchiolar epithelium of the lightly exercising human is estimated to be similar to that in the mainstem bronchi of the spontaneously nose-breathing rat.

Model simulations were also performed at a concentration of 100 ppm. This level causes frank injury in the rat nose and trachea (Hubbs *et al*., 2008) but not small bronchi and bronchioles. Workers were likely transiently exposed to this level in poorly

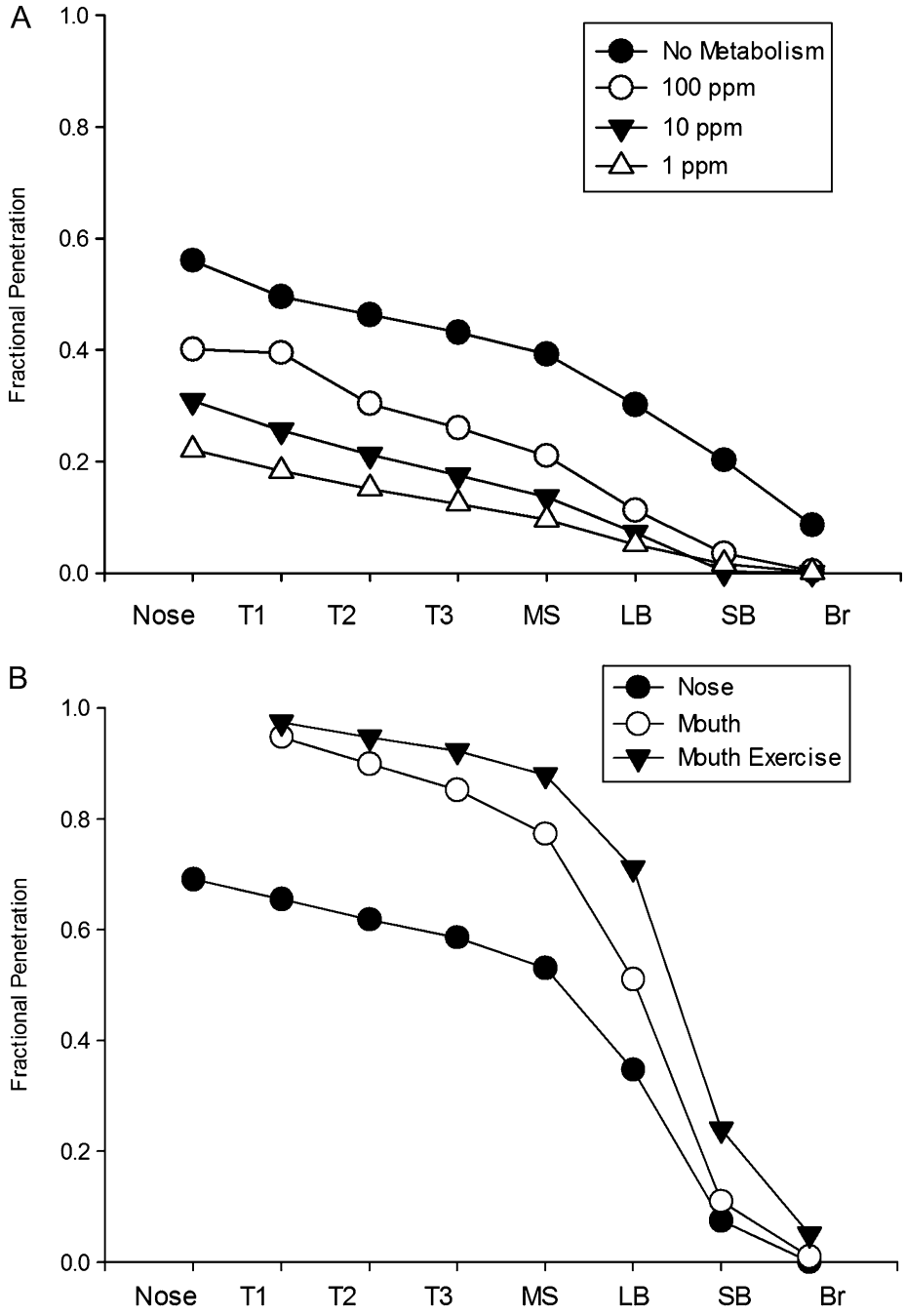

FIG. 6. Penetration of inspired diacetyl to the alveoli. Model estimates for the fraction of inspired diacetyl which penetrates through the designated airway. (Nose = nose, T1 = proximal trachea, T2 = mid trachea, T3 = distal trachea, MS = mainstem bronchi, LB = large bronchi, SB = small bronchi, Br = bronchioles). (A) Model estimates for distal penetration of diacetyl vapor in the rat exposed to 100 ppm with no metabolism or direct reaction, 100, 10, or 1 ppm when metabolism and direct reaction are allowed to occur. (B) Model estimates for distal penetration of 1 ppm diacetyl vapor in the human breathing through the nose (at rest), mouth (at rest), and mouth during light exercise.

ventilated facilities (Akpinar-Elci *et al*., 2004; Kreiss *et al*., 2002). Tissue concentrations in the rat nose and trachea were estimated to be 1100 and 300μM compared with only 3 and 0.3μM in the small bronchi and bronchioles, respectively. In the mouth-breathing lightly exercising human exposed to 100 ppm, tracheal concentrations of 900μM are estimated, values similar to the nose of the rat. (Similar values were obtained regardless of the extrapolation procedure used for metabolism rate.) Small bronchi and bronchiolar tissue concentrations of 300 and 20μM are estimated, values much greater than the rat, and levels that

TABLE 3
Estimated Airway Tissue Concentrations (μM) in the Rat and Human Exposed to 1 ppm Diacetyl[a]

Species breathing route breathing pattern metabolism	Rat nose rest		Human nose rest			Human mouth rest		Human mouth exercise	
	None	*V*max	None	*V*max	*K*cat	*V*max	*K*cat	*V*max	*K*cat
Proximal nose	12	5.4	12	3.4	8.6				
Proximal trachea	6.6	0.33	11	1.1	1.4	1.6	2.0	2.1	2.5
Mainstem bronchi	4.9	0.10	10	0.77	1.0	1.2	1.4	1.7	2.1
Small bronchi	2.5	0.018	5.2	0.10	0.13	0.15	0.18	0.47	0.58
Bronchioles	1.0	0.0022	2.9	0.008	0.011	0.013	0.016	0.07	0.09
ratio: human/rat bronchiole			3×	4×	5×	6×	7×	34×	43×

[a]Estimated tissue concentrations in five respiratory tract airways of the human and rat exposed to 1 ppm diacetyl for 10 min. Estimations were performed assuming no *in situ* respiratory tract metabolism or assuming metabolism rates (expressed per cm^2 surface area, see text) were the same in the rat and human based on the *V*max values obtained for the rat or calculating the rat-human species difference based on the *k*cat values for each species (see text for definitions and details.).

approximate the concentration estimated in the trachea of the rat exposed to 100 ppm.

DISCUSSION

The goals of the current study were (1) to develop a model for total respiratory tract vapor uptake by integrating the concepts of LRT vapor absorption/desorption with the modeling structures used for the URT and (2) to apply this model to gain insights into the inhalation dosimetry of diacetyl (2,3 butanedione). Uptake of inspired vapors is a complex process. Early descriptions assumed that vapors did not absorb in the airways and focused solely on alveolar vapor uptake (Henderson and Haggard, 1943). These resulted in the development of simple ventilation-perfusion models. It is now clear that the conducting airways do not behave as inert tubes and respiratory tract vapor uptake can be strongly influenced by processes within the conducting airways (Gerde and Dahl, 1991; Johanson, 1991; Kumagai and Matsunaga, 2000). Soluble vapors are absorbed in the airway mucus and tissues during inspiration and desorb back into the airspace during exhalation, a process termed washin/washout or vapor recycling. The desorption of vapor into the expired airstream serves to increase end inspired air vapor concentration and diminish overall uptake efficiency because the desorbed vapors are exhaled (Gerde and Dahl, 1991; Johanson, 1991; Kumagai and Matsunaga, 2000). This process is not important for low solubility vapors (blood:air partition coefficient < 10) because little vapor is absorbed into the airways. High solubility vapors (blood:air partition coefficient vapors > 1000), partition effectively into airway tissues but do not effectively desorb (due to their very high partition coefficient), therefore vapor recycling becomes insignificant. This leads to a multiphasic relationship between uptake efficiency and increasing partition coefficient with uptake efficiency (1) increasing as partition coefficient increases from 0 to ~10 (due to increasing alveolar absorption with little airway absorption/desorption), then (2) decreasing as partition coefficient increases from ~10 to ~1000 as airway absorption/desorption becomes more significant, and finally (3) increasing as partition coefficient increases from 1000 to higher levels (as desorption becomes less and less significant). The current model captured this behavior (Fig. 4), providing strong evidence that it captures essential absorption and desorption behaviors. The model also described uptake in the rodent, both uptake within the isolated URT as well as whole respiratory tract uptake of spontaneously breathing rats, with model estimates being within 1 SD of the measured values (Fig. 5). This concordance of model predictions with experimental values in both the human and rat serves to validate the modeling approach. In this regard, it is important to note that every variable has a preassigned value; no variable was altered to enhance the fit to the data.

While the model is validated with respect to experimental measures obtained from exhaled air, it is important to note that the model is not validated with respect to experimental measures of regional absorption within the tracheobronchial tree. This represents a limitation of the current approach. It can be noted, however, that due to its invasive nature, it is not possible to directly measure regional tracheobronchial vapor uptake without introducing considerable artifacts. Another limitation of the model is that the assigned values for some parameters, particularly superficial airway blood flow rates, are somewhat arbitrary. Nonetheless, the closeness of model predictions to experimental values suggests that the assigned parameter values were adequately representative. It should be noted that modeling approaches provide informed estimates but model output should not be construed to represent actual experimental data. The model is focused on inhalation dosimetry during the start of inhalation exposure. As exposures progress, vapor accumulates in systemic tissues leading to systemic blood recirculation to the respiratory tract. Typical respiratory uptake studies for PBPK modeling rely on measurements over several hours of exposure and exclude

early time points. This is necessary because the focus of these studies is to quantify the effect of systemic organ clearance (e.g., liver) on uptake. The focus of the current study was on the early time points because this is when regional respiratory tract dosimetric patterns can be revealed without the confounding influence of systemic events. For highly soluble vapors such as diacetyl, several hours would be expected to be required before significant systemic blood recirculation of vapors occurs. The model could be extended by including whole body PBPK approaches, as has been done for ethyl acrylate (Frederick *et al.*, 2002), if it was desired to model long exposure periods. Finally, it should be noted that the model relied upon CFD predictions for nasal mass transfer coefficient estimates, but a simplified cylindrical tube approach was used for the LRT (see Appendix), thus, it should be recognized that the model structure is not fully CFD based.

Sensitivity analysis provides insights into those factors which strongly influence inhalation dosimetry. In both the rat and human, uptake efficiency diminished with increasing breathing frequency because faster breathing leads to less time for airway absorption. For high partition coefficient (e.g., soluble) vapors, it has long been known that uptake efficiency will depend on cardiac output (Henderson and Haggard, 1943); this was predicted by the model. Local airway perfusion rates also increase uptake efficiency as blood removal from the airways enhances absorption and decreases the amount of vapor available for desorption. The values for local airway perfusion are not known with certainty but were assumed based on estimates of regional perfusion and the split of blood flow to superficial versus deep airway tissues. Better estimates of airway perfusion might improve model estimates. The sensitivity analysis also indicates that uptake efficiency is sensitive to the airway dimension (length, diameter), suggesting that improved values for these parameters (relative to body weight, for example) might improve model predictions and that interindividual variation in these parameters might be important. Model predictions were also sensitive to overall mass transfer coefficient, particularly for the human, again suggesting that improved values might improve model predictions. The model suggests that functional residual capacity is not important. For a vapor of partition coefficient of 500, little penetration to the alveoli is predicted, thus, the independence on functional residual capacity is expected. It is important to note that entirely differing behavior would be anticipated for a low partition coefficient vapor, highlighting that the sensitivity analysis is specific to a vapor with properties similar to diacetyl.

Diacetyl simulations reveal diacetyl uptake efficiency is highly sensitive to *in situ* metabolism rates, as estimated uptake efficiencies of 40% were obtained for the rat assuming no metabolism compared with ~60% if *in situ* metabolism was allowed. The importance of *in situ* metabolism in enhancing airway vapor absorption has long been appreciated (Morris, 1990; Sarangapani *et al.*, 2002). The results of the *in vitro* studies revealed diacetyl was extensively metabolized in all tissues of the respiratory tract. Both a high affinity and low affinity pathway were observed. In this way, diacetyl metabolism appears quite similar to that of acetaldehyde (Morris, 1997) for which both high and low affinity pathways are observed in respiratory tract tissues of multiple species. The identities of the high and low affinity pathways for diacetyl metabolism are not known with certainty. However, the high affinity path was inhibited by sodium benzoate, a known inhibitor of DCXR. The K_m for this path (10μM) differs widely from the K_m reported for cloned/expressed rat DCXR (1.1mM). The reasons for this are not clear. It may represent a strain difference and/or it is possible the K_m of cloned/expressed enzyme differs from that in tissue homogenates. Further studies are needed to resolve this issue. The low affinity pathway demonstrated a high K_m—6.5mM. It is unlikely this pathway contributes significantly to diacetyl metabolism during environmentally relevant exposure scenarios. Even at exposure concentrations of 100 ppm, tissue maximal tissue concentrations of 1.1mM were estimated, levels fivefold below the K_m of this path. Exposure at these levels may induce tissue injury resulting in altered metabolism rates, the current approach did not attempt to model this possibility.

The current results confirm, based on N-acetylarginine dependent disappearance of diacetyl, that diacetyl reacts directly with N-acetylarginine. The reaction rate, however, is slow, averaging less than 0.01/min, even at N-acetylarginine concentrations of 30mM. This is consistent with the results of Mathews *et al.* (2010), whose data suggest that ~50% of diacetyl reacts with N-acetylarginine over a 3-h incubation period. An estimated reaction rate constant of 0.3/min was included in the model. This would be equal to the reaction rate were the tissue substrate concentration 1M. This is also one-tenth of the estimated first order reaction constant for acrolein (Schroeter *et al.*, 2008). It is important to note that at a value of 0.3, inclusion of the first order reaction term had minimal effect (less than a factor of 1.01) on model output. The term was included, however, for the sake of completeness. It is recognized that reactions rates may differ with changes in pH or with substrates other than N-acetylarginine, however, that the model was insensitive to reaction rate indicates the precise value assumed for reaction rate does not markedly affect model predictions. Although not fast enough to strongly influence dosimetric relationships, the reaction of diacetyl with protein arginine residues may be very important toxicologically, as adducts may accumulate slowly, particularly during repeated exposures, and result in immunologic responses (Mathews *et al.*, 2010).

An advantage of developing validated rat and human vapor dosimetry models of identical fundamental structure is that it allows for direct model-based comparisons of the dosimetry of diacetyl in both species. In both species, significant absorption of diacetyl in proximal airways is estimated to occur leading to

limited penetration to the distal airways. This is observed regardless of the specific assumptions made relative to *in situ* metabolism rates. In the absence of metabolism, the model predicts that < 10% penetrates through the bronchioles and reaches the alveoli of the human. This is consistent with the earlier models (Johanson, 1991; Kumagai and Matsunaga, 2000) which predict limited alveolar penetration of vapors with partition coefficients of 500 or greater. Distal penetration of vapors appears to be more limited in the rat than human. In the absence of metabolism, it is estimated that 20% penetrates to the bronchioles of the rat compared with 40% in the human. This is likely the result of many factors. In the human LRT, the epithelium is thicker (leading to a larger air:blood barrier in the airway), the mass transfer coefficients are smaller (leading to less efficient transfer across the air:mucus interface), and the perfusion, expressed as ml/min/cm^2 airway surface area, is smaller than in the rat. Diminished scrubbing of vapors in the nose of the human compared with the rat has been observed previously for multiple vapors including ethyl acrylate, acrylic acid, acrolein, and acetaldehyde (Frederick *et al*., 1998, 2002; Schroeter *et al*., 2008; Teeguarden *et al*., 2008) and is the result of the same multiple factors as enumerated above for the LRT. Increased distal penetration of airborne diacetyl in the human compared with rat lung leads to increased delivered doses to the small airways. Estimated bronchiolar epithelial tissue concentrations (in the absence of metabolism) averaged approximately threefold higher in the nose breathing human at rest than the spontaneously nose-breathing rat at the same inspired concentration.

The difference between the large and small airways and between the human and rat become accentuated when metabolism is allowed. Inclusion of *in situ* metabolism in the rat simulations leads to near total scrubbing of diacetyl in the proximal airways, with only 2% of inspired diacetyl estimated to penetrate to the bronchioles at an inspired concentration of 1 ppm. Estimated bronchiolar tissue concentrations with metabolism allowed are 0.002μm compared with 1.0μM with no metabolism. This is due to the diminished distal penetration with metabolism (as noted above) but also to effective metabolic clearance of diacetyl within the bronchiolar epithelium. At exposure concentrations of 100 ppm, which result in cytotoxic injury in the nose and tracheal (Hubbs *et al*., 2008), concentrations of 1100–300μM are predicted in the nose and trachea of the rat compared with levels of only 0.3μM in the bronchioles. Given this steep gradient in airway epithelial diacetyl concentrations, the absence of injury in the small airways of the rat is, perhaps, not surprising.

Bronchiolar tissue concentrations in the human are estimated to be substantially higher than in the rat exposed to the same concentration. These projections are somewhat limited in that the metabolism rate within human airways is not known with certainty, however, similar patterns are observed if a direct extrapolation of rat metabolism rates is used or if a species-specific *k*cat extrapolation is performed (as described above under diacetyl-specific parameters). The estimated tissue concentrations in the resting nose breathing human are fivefold higher than the spontaneously nose-breathing rat, irrespective of the metabolic extrapolation method that was used. This is in large part due to greater distal penetration of inspired diacetyl in the human than the rat. This suggests that for diacetyl, and perhaps other soluble vapors, the nose breathing rat may underestimate the risks of small airway injury to the human due to differences in inhalation dosimetric patterns. Perhaps, more importantly, humans who are exercising are predicted to be at substantially greater risk than spontaneously nose-breathing rats. Certainly, the concept of increased risk to the small airways in exercising humans is not new (Miller *et al*., 1993). Exercise causes mouth breathing, which eliminates the scrubbing of vapors in upper respiratory tract. Moreover, diminished airway scrubbing and increased distal airway penetration occurs during exercise due to the increased breathing frequency and increased ventilation rates. This results in estimated bronchiolar tissue concentrations in the human during light exercise that exceed those in the rat by 40-fold. Analogous predictions have been made for ozone dosimetry (Miller *et al*., 1993). For diacetyl, the estimated bronchiolar tissue concentrations in the human during light exercise were similar to those estimated for the main stem bronchi of the spontaneously breathing rat exposed to the same concentration (1 ppm). Quantitatively similar estimates were obtained regardless of the extrapolation procedure used for human metabolism rate. Given the proportionately large delivered dosage rate in the bronchiolar epithelium, it is perhaps not surprising that injury results in this site in the human. The observation of bronchiolar injury in rodent models in which diacetyl is delivered to the small airways via instillation, documents these airways are sensitive to diacetyl if local delivery rates are sufficiently high (Palmer *et al*., 2011). Precise comparisons among airways would require information on the sensitivity of bronchial versus bronchiolar epithelium in the human and rat to diacetyl-induced injury. Importantly, the model simulations provide evidence that the delivered dosage rates and tissue concentrations in the bronchiolar airways of the exercising human may be significantly greater than in the rat. In this regard, inhalation toxicity testing which relies on the spontaneously breathing rat may not be predictive of injury that may result in the exercising human. This certainly appears to be the case for diacetyl, in which a discordance of target sites is seen in the human versus the rat (Akpinar-Elci *et al*., 2004; Hubbs *et al*., 2008; Kreiss *et al*., 2002) as well as a discordance in delivered dose as predicted by the model simulations described herein. This may generally be the case for other soluble vapors as well. If so, appropriate interpretation of rodent toxicity data requires appropriate dosimetric extrapolation which, in particular, considers relationships between the spontaneously nose-breathing rodents used in inhalation toxicity testing and mouth-breathing exercising humans.

ACKNOWLEDGMENTS

John Morris has served as a consultant to ConAgra on diacetyl toxicity.

APPENDIX

The hybrid CFD-PBPK model for lower airway dosimetry was based on the URT PBPK approach developed in this laboratory (Morris *et al*., 1993) incorporating the CFD components described by Frederick *et al*. (1998). This general structure is shown in Figures 1 and 2. This structure has been widely used and validated relative to URT dosimetry for a variety of vapors (see text). The model structure consists of a moving airstream that passes over respiratory tissues that are modeled as stacks of tissue, the dimensions of which are anatomically defined. Airborne vapor was allowed to diffuse into the mucous lining layer in accordance with mass transfer theory and vapor was allowed to diffuse between tissue compartments in accordance with its diffusivity. Direct reaction of vapor with tissue substrates and/or metabolism rates are incorporated into each compartment as appropriate.

The anatomical parameters for the URT are identical to those used previously (Morris and Hubbs, 2009). Shown in Table A1 are the anatomical parameters for the lower airways. The same fundamental structure was used for the rat and human models. The lower airways were modeled as seven airway tissue stacks. Three stacks for the trachea, followed by tissue stacks representing the main bronchi, large bronchi (generations 3–7), small bronchi (generations 8–12), bronchioles (generations 13–16), and alveoli. The anatomical parameters for these airways are shown in Table A1. These were derived from the models of Yeh and coworkers as described by McBride (1992). For the lumped airway stacks (large bronchi, small bronchi, bronchioles), the diameter represents the diameter of the lowest airway in the lumped group (generation 7, 12, and 16 for large bronchi, small bronchi, and bronchioles, respectively). The surface area represents the sum of the surface areas for each of the airways lumped into each designation, and the length is the value calculated to provide the total surface area based on the assumed diameter (see text for details). The alveoli (not shown) are assumed to have a functional residual capacity of 2700 ml for the human (Kumagai and Matsunaga, 2000) and 6.8 ml/kg for the rat (Lai *et al*., 2000).

Also shown in Table 1 are the airway perfusion rates. These were calculated assuming 1.0% of the total cardiac output perfuses the superficial layers of the airways (see text) and then distributed among the airways assuming each airway is perfused in proportion to its surface area (see text). The perfusion of the alveoli is assumed to equal the cardiac output. Based on the equation provided by Frederick *et al*. (1998), a cardiac output 5404 and 92.3 ml/min is estimated, respectively, for the human and rat.

All airways were assumed to be covered by a mucus lining layer of 0.010 mm in depth. The epithelial cell layer depth of each airway was based on measurements in either the human (or monkey) or rat (Mariassy, 2000; Plopper and Hyde, 1992). For the human, the total epithelial depth of the trachea, mainstem bronchi, and large bronchi was assumed to by 0.04 mm and was modeled as four consecutive 0.01-mm compartments. The small bronchi epithelial depth was assumed to be 0.03 mm (three 0.01-mm compartments) and the bronchiolar epithelial depth was assumed to be 0.02 mm (two 0.001-mm compartments). The airway epithelium of the rat is less deep than the human (Mariassy, 2000) and was modeled as 0.020-mm deep in the trachea (two 0.010-mm compartments) and 0.010 mm deep in all other airways (one 0.010-mm compartment). In all airways, a submucosal depth of 0.02 mm was assumed (two 0.01-mm compartments). Blood perfused only the submucosal layer, the perfusion rates for each modeled airway are provided in Table A1.

Transfer of vapor between the air and mucus phases was modeling based on mass transfer approaches using the mass transfer coefficients provided by Frederick *et al*. (1998) for the URT and the approach of Sarangapani *et al*. (2002) for the lower airways. This formulation uses an air diffusivity of 6 cm^2/min (Cussler, 1997) to estimate the air-phase mass transfer coefficient by the formula $MTC_A = 1.62\ (D^2v/Ld)^{1/3}$, where D is the air-phase diffusivity in cm^2/min, v is that average fluid velocity in cm/min, L is the airway length and d is the airway diameter (Cussler, 1997; Sarangapani *et al*., 2002). The overall mass transfer coefficient, Kg, is given by the relationship: $1/Kg = 1/MTC_A + 1/MTC_T \times$ partition coefficient (USEPA, 1994). [An alternate approach for Kg estimation is provided by Condorelli and George (1999) (Condorelli and George, 1999). This approach likely provides a better reflection of flow patterns in branching airways but relies on vapor specific empirical parameters and is not easily amenable for use for a variety of vapors of differing partition coefficient. Using this formulation as developed for ethanol to estimate Kg values for the current model provides predictions similar to those obtained with the Sarangapani *et al*. (2002) (Sarangapani *et al*., 2002) approach (data not shown)]. Once in mucus, vapor was allowed to diffuse into the underlying tissues. The diffusivity in mucus was assumed to equal that in water as was estimated from the ethanol water diffusivity as described by Morris *et al*. (1993). Based on the higher viscosity of tissues relative to water, the tissue diffusivity was assumed to be fourfold lower than that in mucus (Bush *et al*., 1998; Morris *et al*. 1993).

For a metabolized and reactive vapor such as diacetyl, it is necessary that metabolism and reaction rates be included in the tissue phases. The values for these parameters are provided in the text. Reaction was modeled as a pseudo-first order process and was allowed in mucus and all tissue compartments. It should be noted that the reaction rates of diacetyl as determined in the current study were not sufficiently large to exert a significant effect on model predictions; the reaction rate constant was included for the sake of completeness. Metabolism was assumed to follow Michaelis-Menten kinetics and was allowed in only the epithelial compartments as DCXR expression appears to be limited to these cells (Gardiner *et al*., 2009). *In vitro studies* revealed the existence of both high and low affinity metabolic pathways; therefore, two metabolic terms were included in each cellular layer. As noted in the text, the low affinity pathway would not be expected to contribute to diacetyl dosimetry at typical exposure levels but was included for the sake of completeness.

The CFD-PBPK model consists of a series of mass balance differential equation. The mass balance equation for vapor in each airway lumen was identical to that described by Teeguarden *et al*. (2008):

$$V_l dC_l/dt = Q_a(C_{in} - C_l) - K_{lt}(C_l - C_t/H_{ta}),$$

Where V_l is the volume of the airway lumen over each tissue stack, C_l and C_t are the vapor concentration in the airway lumen and mucus compartment, C_{in} is the vapor concentration in air entering the airway lumen, Q_a is airflow over the mucus compartment, H_{ta} is the air:mucus partition coefficient (assumed to be equal to the blood:air partition coefficient), K_{lt} is the lumen to tissue overall mass transfer coefficient, calculated as described above.

As an example, the mass balance equation for vapor in a deep epithelial compartment (E2), which is immediately below the E1 epithelial compartment and immediately above the S1 submucosal compartment, is given by:

$$V_t C_{e2}/dt = kb^* V_t^* (C_{e1} - C_{e2}) + kb^* V_t^* (C_{s1} - C_{e2}) - V^*_{maxe2}\left[C_{e2}/(C_{e2} + K_m)\right] + V^*_{maxe2L}\left[C_{e2}/(C_{e2} + K_{mL})\right] + K_1^* V_t^* C_{e2},$$

Where V_t is the volume of the tissue compartment (all tissue compartments of a stack are of the same volume), kb governs the diffusion between compartments (as described by Morris *et al*., 1993), C_{e1}, C_{e2}, and C_{s1} are the concentrations in the superficial and deep epithelial and superficial submucosal compartments, respectively (see Fig. 1B), and, V_{maxe2} and K_m are the Michealis-Menten constants for the high affinity pathway, and V_{maxe2L} and K_{mL} are the Michaelis-Menton constants for the low affinity pathway, and K_1 is the pseudo-first order rate constant for direct reactivity.

TABLE A1
Anatomical and Physiological Parameters for the Lower Airway Model[a]

Parameter	Trachea	Airway mainstem bronchi	Large bronchi	Small bronchi	Bronchioles
Human					
Number	1	2	64	2048	32,768
Surface area (cm^2)	63	43	213	1445	3033
Length (cm)	10	4.36	2.43	1.44	0.491
Diameter (cm)	2.01	1.56	0.435	0.156	0.060
Lumen volume (cm^3)	32	16	23.1	56.4	45.5
Epithelial depth (mm)	0.040	0.040	0.040	0.030	0.020
Perfusion (ml/min)	0.70	0.48	2.00	16.3	34.2
Overall *Kg* (cm/min)	46.1	43.3	57.7	60.08	84.07
Rat					
Number	1	2	23	309	2487
Surface area (cm^2)	2.86	1.30	4.09	10.7	39.5
Length (cm)	2.68	0.715	0.460	0.158	0.253
Diameter (cm)	0.34	0.29	0.123	0.070	0.020
Lumen volume (cm^3)	0.243	0.0945	0.126	0.188	0.198
Epithelial depth (mm)	0.020	0.010	0.010	0.010	0.010
Perfusion (ml/min)	0.0152	0.0206	0.0652	0.171	0.628
Overall *Kg* (cm/min)	99.6	99.8	113	117	149

[a]Unless otherwise indicated the values are those for the sum of all of the airways in each modeled generation. The values for an individual airway would be obtained by dividing the shown value by the number of airways in that generation. The exceptions are the overall *Kg* and the epithelial depth, the values of which represent the value used for each individual airway. The total cardiac output of the human and rat are estimated to be 5404 and 93.2 ml/min, respectively. The LRT deadspace is estimated to be 173 and 0.85 ml, and the total LRT airway surface area is estimated to be 4797 and 58 cm^2, in the human and rat, respectively.

REFERENCES

Akpinar-Elci, M., Travis, W. D., Lunch, D. A., and Kreiss, K. (2004). Bronchiolitis obliterans syndrome in popcorn production plant workers. *Eur. Respir. J.* **24,** 298–302.

Brown, R. P., Delp, M. D., Lindstedt, S. L., Rhomberg, L. R., and Beliles, R. P. (1997). Physiological parameter values for physiologically based pharmacokinetic models. *Toxicol. Ind. Health* **13,** 407–484.

Bush, M. L., Frederick, C. B., Kimbell, J. S., and Ultman, J. S. (1998). A CFD-PBPK hybrid model for simulating gas and vapor uptake in the rat nose. *Toxicol. Appl. Pharmacol.* **150,** 133–145.

Carbone, V., Ishikura, S., Hara, A., and El-Kabbani, O. (2005). Structure-based discovery of human L-xylulose reductase inhibitors from database screening and molecular docking. *Bioorg. Med. Chem.* **13,** 301–312.

Condorelli, P., and George, S. C. (1999). Theoretical gas phase mass transfer coefficients for endogenous gases in the lungs. *Ann. Biomed. Eng.* **27,** 326–339.

Cussler, E. L. (1997). In *Diffusion: Mass Transfer in Fluid Systems*, 2nd ed. Cambridge University Press, New York, NY.

Fiserova-Bergerova, V. (1983). Gases and their solubility: a review of the fundamentals. In *Modeling of Inhalation Exposure to Vapors: Uptake, distribution and Elimination* (V. Fiserova-Bergerova, Ed.), pp. 3–29. CRC Press, Boca Raton, FL.

Frederick, C. B., Bush, M. L., Lomax, L. G., Black, K. A., Finch, L., Kimbell, J. S., Morgan, K. T., Subramaniam, R. P., Morris, J. B., and Ultman, J. S. (1998). Application of a hybrid computational fluid dynamics and physiologically based inhalation model for interspecies dosimetry extrapolation of acidic vapors in the upper airways. *Toxicol. Appl. Pharmacol.* **152,** 211–231.

Frederick, C. B., Gentry, P. R., Bush, M. L., Lomax, L. G., Black, K. A., Finch, L., Kimbell, J. S., Morgan, K. T., Subramaniam, R. P., Morris, J. B., *et al.* (2001). A hybrid computational fluid dynamics and physiologically based pharmacokinetic model for comparison of predicted tissue concentrations of acrylic acid and other vapors in the rat and human nasal cavities following inhalation exposure. *Inhal. Toxicol.* **13,** 359–376.

Frederick, C. B., Lomax, L. G., Black, K. A., Finch, L., Scribner, H. E., Kimbell, J. S., Morgan, K. T., Subramaniam, R. P., and Morris, J. B. (2002). Use of a hybrid computational fluid dynamics and physiologically based inhalation model for interspecies dosimetry comparisons of ester vapors. *Toxicol. Appl. Pharmacol.* **183,** 23–40.

Gardiner, D. W., Goldsmith, W. T., Morris, J. B., Battelli, L. A., Friend, S., Castranova, V., and Hubbs, A. F. (2009). Adhesion molecule expression and cytotoxicity in diacetyl exposed Rat lungs. *Toxicologist* **108,** 432.

Gerde, P., and Dahl, A. R. (1991). A model for the uptake of inhaled vapors in the nose of the dog during cyclic breathing. *Toxicol. Appl. Pharmacol.* **109,** 276–288.

Henderson, Y., and Haggard, H. W. (1943). In *Noxious Gases and the Principles of Respiration Influencing Their Action*. Reinhold, New York, NY.

Hinderliter, P. M., Thrall, K. D., Corley, R. A., Bloemen, L. J., and Bogdanffy, M. S. (2005). Validation of human physiologically based pharmacokinetic model for vinyl acetate against human nasal dosimetry data. *Toxicol. Sci.* **85,** 460–467.

Hubbs, A. F., Battelli, L. A., Goldsmith, W. T., Porter, D. W., Frazer, D., Friend, S., Schwegler-Berry, D., Mercer, R. R., Reynolds, J. S., Grote, A., *et al.* (2002). Necrosis of nasal and airway epithelium in rats inhaling vapors of artificial butter flavoring. *Toxicol. Appl. Pharmacol.* **185,** 128–135.

Hubbs, A. F., Goldsmith, W. T., Kashon, M. L., Frazer, D., Mercer, R. R., Battelli, L. A., Kullman, G. J., Schwegler-Berry, D., Friend, S., and Castranova, V. (2008). Respiratory toxicologic pathology of inhaled diacetyl in sprague-dawley rats. *Toxicol. Pathol.* **36,** 330–344.

Johanson, G. (1991). Modelling of respiratory exchange of polar solvents. *Ann. Occup. Hyg.* **35,** 323–339.

Kety, S. (1951). The theory and applications of the exchange of inert gas at the lungs and tissues. *Pharmacol. Rev.* **3,** 1–42.

Kimbell, J. S., Gross, E. A., Joyner, D. R., Godo, M. N., and Morgan, K. T. (1993). Application of computational fluid dynamics to regional dosimetry of inhaled chemicals in the upper respiratory tract of the rat. *Toxicol. Appl. Pharmacol.* **121,** 253–263.

Kreiss, K., Gomaa, A., Kullman, G., Fedan, K., Simoes, E. J., and Enright, P. L. (2002). Clinical bronchiolitis obliterans in workers at a microwave-popcorn plant. *N. Engl. J. Med.* **347,** 330–338.

Kumagai, S., and Matsunaga, I. (2000). A lung model describing uptake of organic solvents and roles of mucosal blood flow and metabolism in the bronchioles. *Inhal. Toxicol.* **12,** 491–510.

Lai, Y.-L. (1992). Comparative ventilation of the normal lung. In *Comparative Biology of the Normal Lung* (R. A. Parent, Ed.), pp. 219–239. CRC Press, Boca Raton, FL.

Mariassy, A. T. (1992). Epithelial cells of the trachea and bronchi. In *Comparative Biology of the Normal Lung* (R. A. Parent, Ed.), pp. 63–83. CRC Press, Boca Raton, FL.

Martin, A., Swarbrick, J., and Cammarate, A. (1983). In *Physical Pharmacy: Physical Chemical Principles in the Pharmaceutical Sciences*. Lea & Febiger, Philadelphia, PA.

Mathews, J. M., Watson, S. L., Snyder, R. W., Burgess, J. P., and Morgan, D. L. (2010). Reaction of the butter flavorant diacetyl (2,3-butanedione) with N-alpha-acetylarginine: a model for epitope formation with pulmonary proteins in the etiology of obliterative bronchiolitis. *J. Agric. Food Chem.* **58,** 12761–12768.

McBride, J. T. (1992). Architecture of the tracheobronchial tree. In *Compartative Biology of the Normal Lung* (R. A. Parent, Ed.), pp. 49–61. CRC Press, Boca Raton, FL.

Medinsky, M. A., Bond, J., Schlosser, P. M., and Morris, J. B. (1999). Mechanisms and models for respiratory tract uptake of volatile organic compounds. In *Toxicology of the Lung* (D. W. Gardiner, J. E. Crapo, and R. O. McClellan, Eds.), pp. 483–512. Taylor and Francis, Philadelphia, PA.

Meulenberg, C. J., Wijnker, A. G., and Vijverberg, H. P. (2003). Relationship between olive oil:air, saline:air, and rat brain:air partition coefficients of organic solvents in vitro. *J. Toxicol. Environ. Health Part A* **66,** 1985–1998.

Miller, F. J., Overton, J. H., Kimbell, J. S., and Russell, M. L. (1993). Regional respiratory tract absorption of inhaled reactive gases. In *Toxicology of the Lung* (D. J. Gardner, J. E. Crapo, and R. O. McLellan, Eds.), pp. 485–525. Raven Press, New York, NY.

Morgan, D. L., Flake, G. P., Kirby, P. J., and Palmer, S. M. (2008). Respiratory toxicity of diacetyl in C57BL/6 mice. *Toxicol. Sci.* **103,** 169–180.

Morris, J. B. (1990). First-pass metabolism of inspired ethyl acetate in the upper respiratory tracts of the F344 rat and Syrian hamster. *Toxicol. Appl. Pharmacol.* **102,** 331–345.

Morris, J. B. (1997). Uptake of acetaldehyde vapor and aldehyde dehydrogenase levels in the upper respiratory tracts of the mouse, rat, hamster, and guinea pig. *Fundam. Appl. Toxicol.* **35,** 91–100.

Morris, J. B., and Buckpitt, A. R. (2009). Upper respiratory tract uptake of naphthalene. *Toxicol. Sci* **111,** 383–391.

Morris, J. B., and Cavanagh, D. G. (1986). Deposition of ethanol and acetone vapors in the upper respiratory tract of the rat. *Fundam. Appl. Toxicol.* **6,** 78–88.

Morris, J. B., Clay, R. J., and Cavanagh, D. G. (1986). Species differences in upper respiratory tract deposition of acetone and ethanol vapors. *Fundam. Appl. Toxicol.* **7,** 671–680.

Morris, J. B., Hassett, D. N., and Blanchard, K. T. (1993). A physiologically based pharmacokinetic model for nasal uptake and metabolism of non-reactive vapors. *Toxicol. Appl. Pharmacol.* **123,** 120–129.

Morris, J. B., and Hubbs, A. F. (2009). Inhalation dosimetry of diacetyl and butyric acid, two components of butter flavoring vapors. *Toxicol. Sci.* **108,** 173–183.

Morris, J. B., Kimbell, J. S., and Asgharian, B. (2010). Upper airway dosimetry of gases, vapors and particulate matter in rodents. In *Toxicology of the Nose and Upper Airway* (J. B. Morris and D. J. Shusterman, Eds.), pp. 99–115. Informa Healthcare, New York, NY.

Nakagawa, J., Ishikura, S., Asami, J., Isaji, T., Usami, N., Hara, A., Sakurai, T., Tsuritani, K., Oda, K., Takahashi, M., *et al.* (2002). Molecular characterization of mammalian dicarbonyl/L-xylulose reductase and its localization in kidney. *J. Biol. Chem.* **277,** 17883–17891.

Palmer, S. M., Flake, G. P., Kelly, F. L., Zhang, H. L., Nugent, J. L., Kirby, P. J., Foley, J. F., Gwinn, W. M., and Morgan, D. L. (2011). Severe airway epithelial injury, aberrant repair and bronchiolitis obliterans develops after diacetyl instillation in rats. *PLoS One* **6,** e17644.

Paredi, P., and Barnes, P. J. (2009). The airway vasculature: reent advances and clinical implications. *Thorax* **64,** 444–450.

Plopper, C., and Hyde, D. M. (1992). Epithelial cells of the bronchioles. In *Comparative Biology of the Normal Lung* (R. A. Parent, Ed.), pp. 85–92. CRC Press, Boca Raton, FL.

Plowchalk, D. R., Andersen, M. E., and Bogdanffy, M. S. (1997). Physiologically based modeling of vinyl acetate uptake, metabolism, and intracellular pH changes in the rat nasal cavity. *Toxicol. Appl. Pharmacol.* **142,** 386–400.

Poulin, P., and Krishnan, K. (1995). An algorithm for predicting tissue: blood partition coefficients of organic chemicals from n-octanol: water partition coefficient data. *J. Toxicol. Environ. Health* **46,** 117–129.

Sarangapani, R., Teeguarden, J. G., Cruzan, G., Clewell, H. J., and Andersen, M. E. (2002). Physiologically based pharmacokinetic modeling of styrene and styrene oxide respiratory-tract dosimetry in rodents and humans. *Inhal. Toxicol.* **14,** 789–834.

Schroeter, J. D., Kimbell, J. S., Gross, E. A., Willson, G. A., Dorman, D. C., Tan, Y. M., and Clewell, H. J., 3rd. (2008). Application of physiological computational fluid dynamics models to predict interspecies nasal dosimetry of inhaled acrolein. *Inhal. Toxicol.* **20,** 227–243.

Stott, W. T., Dryzga, M. D., and Ramsey, J. C. (1983). Blood-flow distribution in the mouse. *J. Appl. Toxicol.* **3,** 310–312.

Teeguarden, J. G., Bogdanffy, M. S., Covington, T. R., Tan, C., and Jarabek, A. M. (2008). A PBPK model for evaluating the impact of aldehyde dehydrogenase polymorphisms on comparative rat and human nasal tissue acetaldehyde dosimetry. *Inhal. Toxicol.* **20,** 375–390.

USEPA. (1994). *Methods for Derivation of inhalation Reference concentrations and application of inhalation dosimetry*. U.S. EPA Office of Health and Environmental assessment, Washington, DC.

Yeh, H. C., and Schum, F. M. (1980). Models of human lung airways and their application to inhaled particle deposition. *Bull. Math. Biol.* **42,** 461–480.

Yeh, H. C., Schum, F. M., and Duggan, M. T. (1979). Anatomic models of the tracheobronchial and pulmonary regions of the rat. *Anat. Rec.* **195,** 482–492.